

Original Article

Expression of AQP3 in the mice endometrium during estrous cycle and early pregnancy

Dan Cui*, Linlin Sui*, Chenyang Zhu, Yanni Ma, Man Zhang, Zhenzhen Guo, Yunpeng Xie, Ying Kong

Department of Biochemistry and Molecular Biology, Dalian Medical University, Dalian 116044, Liaoning, China.

**Equal contributors.*

Received April 6, 2016; Accepted June 13, 2016; Epub August 1, 2016; Published August 15, 2016

Abstract: The rodents' uterus undergoes extensive morphologic changes for embryo implantation. Uterine edema is a general feature in the peri-implantation period of rodents. Uterine swelling facilitates closure of the uterine lumen around the free-floating blastocyst. In the absence of a blastocyst the uterine becomes ultimately a closing down of the lumen, but the mechanisms that regulate fluid transport during implantation are not fully understood. To determine the presence and distribution of aquaporin3 (AQP3) in mouse uterine tissue, experimental manipulation of AQP3 activities was performed in vivo. Histological examination of endometrial tissues was performed throughout the estrous cycle and early pregnancy. In this study, we showed that AQP3 immunoreactivity was located in the stromal cells and the expression levels increased from the metestrous to proestrous phase. Additionally, the results of Gross anatomic of uteri and immunohistochemistry showed endometrial thickening, uterine edema, and an enlarged uterine cavity gap in the proestrous and estrous of mice. In early pregnancy, intense staining for AQP3 was seen in the stromal cells of D5 uterine tissue sections, with its localization intensely confined in the cells surrounding implantation site. On day 8 of pregnancy, AQP3 showed no obvious expression in the uterine decidual tissue. However, AQP3 expression showed a specific increase in the uterine stromal cells around the non-attachment site of embryo implantation. This result suggests that AQP3 may play a role in stromal edema, uterine closure and uterine fluid homeostasis during implantation.

Keywords: AQP3, estrous cycle, implantation, decidualization

Introduction

Uterine edema is a general feature of implantation in rodents, nonhuman primates, and humans [1, 2]. On the progress of embryo implantation, AQPs mediate water imbibitions and movement of water into the luminal cavity of the uterus. Water moves across the cell not only by permeating through the membrane lipid bilayer but also through water channels protein (WCPs). Water channel proteins (Aquaporins, Aqps) widely expressed in prokaryotic and eukaryotic cell membranes remains open and do not need energy consumption to rapid transport water and glycerin molecules. In mammals, there are 13 kinds of subtypes AQPs (AQPO-AQP12), which show a wide range of distribution in different organs [3]. According to their structural and functional properties, AQPs are divided into three subgroups: aquaporins (AQPs), aquaglyceroporins, and S-aquaporins.

AQPO, 1, 2, 4, 5, 6 and 8, belonging to classical aquaporins, are water-selective channels permeable to water but not to small organic and inorganic molecules. Based on their sequences, AQP6 (also permeable to anions) and AQP8 (also permeable to urea) can also be included in this subgroup [4, 5]. AQP3, 7, 9, and 10, belonging to aquaglyceroporins, are nonselective water channels permeable to glycerol, urea, other small nonelectrolytes, and water [6]. AQP9 also facilitates the flux of neutral solutes such as monocarboxylates, purines and pyrimidines [7, 8]. The remaining two members, AQP11 and 12, belonging to the third subfamily, are named by various authors as "super-aquaporins", which are localized in the cytoplasm and whose permeabilities have not yet been fully determined [9, 10].

Further studies report that AQP4-deficient mice are sub-fertile [11], however AQP8-deficient

Function of AQP3 in the mice endometrium

mice have higher than normal fertility [12]. AQP7 is important in uterine decidualization, which might transport glycerol as an extra energy source in the process. The studies of Richard et al found that AQP0, AQP1 and AQP3~AQP9 are expressed in the CD1 mice uterus. AQP4 expression is highest in the luminal epithelium at D1 of pregnancy (AQP4 is only expressed in the luminal epithelium at D1), whereas AQP4 showed no obvious expression in the uterine at the time of implantation [13]. It is found that AQP1 was present in the myometrium of the pregnant rat uterus with the intensity of AQP1 immunore activity increasing from day 1 to day 6 of pregnancy. It is suggested that AQP1 plays a role in stromal edema, uterine closure and orientation of the blast cyst [14]. AQP5 and AQP9 are weakly expressed in the uterine glandular epithelium in early pregnancy; however, after blast cyst attachment, AQP5 and AQP9 expression are markedly increased. AQP5 is dependent on estrogen stimulation of the progesterone-primed uterus [15]. Research indicate that the promoter of AQP5 gene contains a functional estrogen response element (ERE) motif, which may mediate estrogen-induced up regulation of AQP5 expression [16]. The presence of uterine edema before implantation, the uterine contraction after blast cyst attachment, and the rapid onset of highly localized vascular permeability surrounding the implanting mouse blastocyst suggest that AQPs might regulate tissue fluid balance during implantation. Aquaporin3 was also only found in the mouse uterus in ovariectomized control and estrogen treated animals [17]. Microarray studies suggest that AQP3 is present in human uterine luminal epithelial cells [18].

The present study investigates the distribution of AQP3 expression in the mice uterus during the estrous cycle and early pregnancy, and the distribution of AQP3 expression in the uterine decidualization and the non-attachment site of embryo implantation and the attachment site.

Materials and methods

Animals and treatments

Mice of Kunming species were approved by the Institutional Review Board on the Use of Live Animal in Teaching and Research, the Dalian Medical University. The mice were housed in a temperature 22-25°C, humidity 60%, and light-

controlled (12 h light: 12 h darkness) with ad libitum access to water and food. Adult female mice weighted 20-24 g and adult male mice weighted 40-44 g was maintained under controlled environmental conditions.

The mouse which the estrous cycle was determined by a vaginal smear was immediately killed to collect its uterus. Adult female mice, which were intended to be the estrous phase, were mated with fertile males of the same strain to induce natural pregnancy. Pregnancy was ascertained on days 1 (D1 = day of vaginal plug) by recovering embryos from the oviduct. The implantation sites on D5 and D8 were identified by intravenous injection of 0.1 ml of 1% Chicago blue in saline (Sigma-Aldrich Co. LLC, Louis, MO, USA). The entire uteri of pregnant mice on D1 and D5 of pregnancy were collected immediately after the mice were sacrificed by cervical dislocation.

Vaginal cytology method

Absorbent cotton swab wetted with ambient temperature physiological saline inserted into the vagina of the restrained mouse. The swab was gently turned and rolled against the vaginal wall and then removed. Vaginal cells were transferred to a dry glass slide by rolling the swab. The slide was natural air dried and fixed with 95% ethanol for 10 min. Then the stage of the estrous cycle was determined based on the presence or absence of leukocytes, cornified epithelial, and nucleated epithelial cells by hematoxylin-eosin (HE) staining. The slides were overlaid with a coverslip, and viewed immediately at 400× magnification under bright field illumination.

Immunohistochemistry

Uterine tissues were dipped in 4% (v/v) paraformaldehyde (Sinopharm Chemical Reagent, Shanghai, China) in PBS (pH 7.4) for 24 h at 4°C and then dehydrated in sucrose. The frozen sections of uteri were cut at a thickness of 5 µm and were blocked with 4% paraformaldehyde for 15 min at room temperature and washed in PBS. Endogenous peroxidase activity was blocked with 3% H₂O₂ for 15 min at room temperature. The sections were then washed in PBS, and incubated in 5% goat serum at 37°C for 15 min. The sections were incubated with rabbit anti AQP3 (1:100; Abcam) overnight at 4°C. After being washed three times with PBS,

Function of AQP3 in the mice endometrium

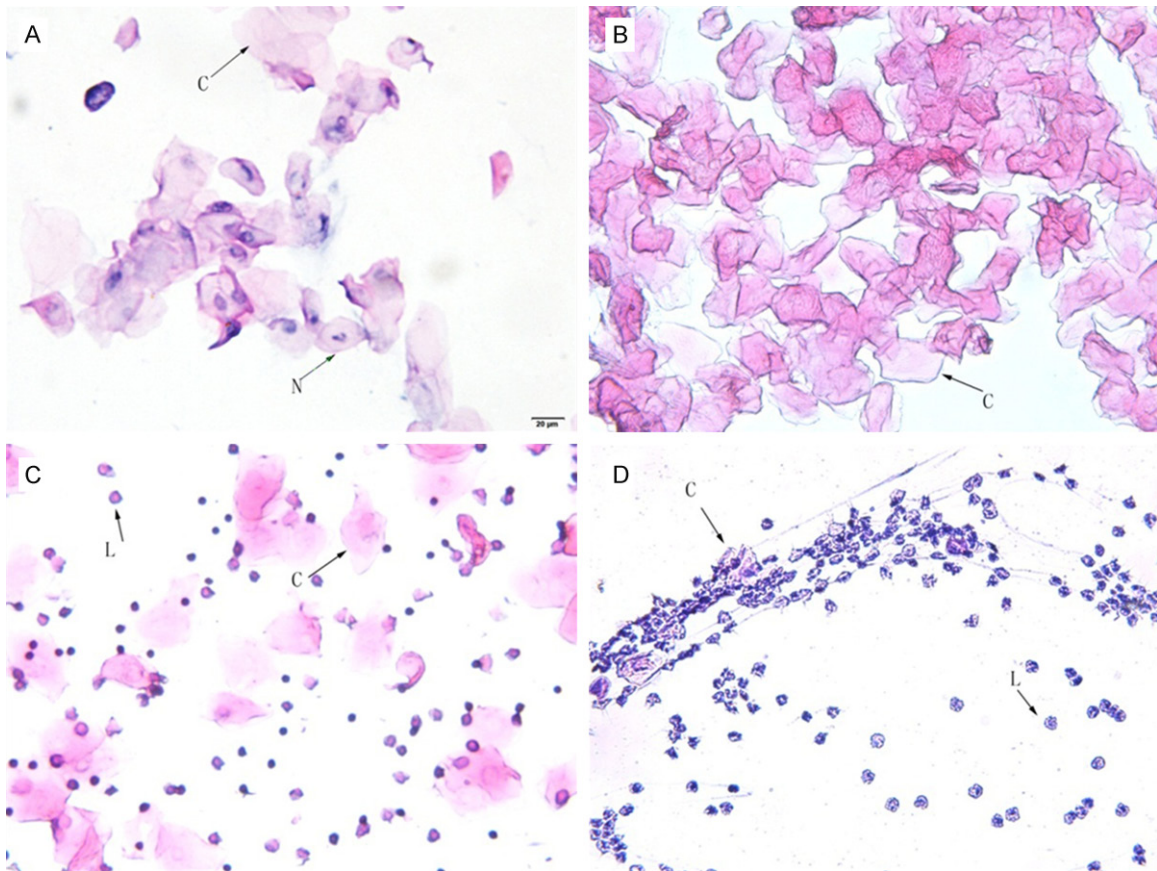


Figure 1. Vaginal cytology representing each stage of estrous by HE staining. Stages of estrous include proestrus (A), estrus (B), metestrus (C), diestrus (D). Three cell types are identified: leukocytes (L), cornified epithelial (C), and nucleated epithelial (N).

sections were incubated with a biotinylated secondary antibody (ZSGB-Bio Co., Ltd., Beijing, China) at 37°C for 40 min. And sections were washed with PBS, and then they were incubated with streptavidin-horseradish peroxidase (ZSGB-Bio, Beijing, China) at 37°C for 40 min. Positive reactions were visualized with a diaminobenzidine (DAB)-peroxidase substrate (ZSGB-Bio, Beijing, China) and counterstaining with haematoxylin for 30 s. Photomicrographs were taken by using an OLYMPUS TH4 microscope. PBS was used as a negative control primary antibody.

RNA extraction and real-time reverse transcription plus polymerase chain reaction

Total RNA was extracted with the TRIzol (Takara, Dalian, China) reagent according to the manufacturer's protocol, and RNA samples were quantified by the measurement of the optic absorbance at 260 and 280 nm with a resul-

tant A260/A280 ratio that ranged from 1.8 to 2.0, which indicated a high purity of the extracted RNA. The concentration of total RNA was calculated according to A260. Aliquots of total RNA (1.0 µg each) from each sample were reverse transcribed into cDNA according to the instructions of the PrimeScript RT Reagent Kit (Takara, Dalian, China). Real-time polymerase chain reaction (PCR) was performed in an ABI Step One Plus Real-time PCR system according to the manufacturer's recommendations. The real-time PCR contained 10 µl 2× SYBR Premix Ex Taq, 0.8 µl primer mix (10 µM), 0.4 µl 50× ROX Reference Dye II, 4 µl cDNA, and 4.8 µl deionized water to make a total volume of 20 µl. The relative amount of specific mRNA was normalized to GAPDH (D-glyceraldehyde-3-phosphate dehydrogenase). All PCRs were run in triplicate and were performed over 40 cycles. Analysis of the results was carried out by using the 2- $\Delta\Delta C_t$ method. The primers used were as follows: AQP3 primer forward: 5'-AACTTGGCT-

Function of AQP3 in the mice endometrium

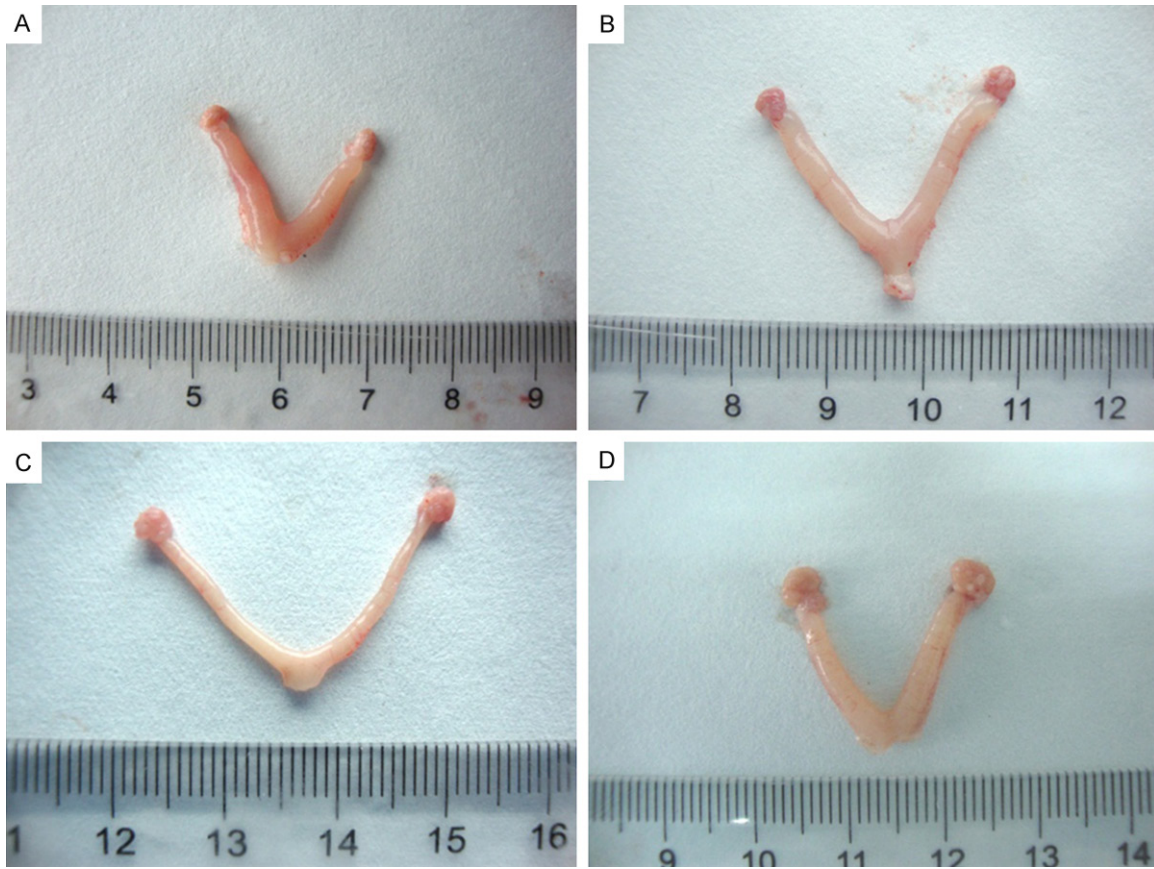


Figure 2. Gross anatomy of uteri during estrous cycle. Stages of estrous include proestrus (A), estrus (B), metestrus (C), diestrus (D).

TTGGCTTCGC-3' and reverse 5'-GGCCAGATTGCATCGTAGT-3'; GAPDH primer forward: 5'-GGTTGTCTCCTGCGACTTCAACAGC-3' and reverse 5'-CGAGTTGGGATAGGGCCTCTCTTGC-3'.

Western blotting

Proteins from uterine tissues or cells were extracted using Lysis Buffer (KeyGen Biotech Co., Ltd., Nanjing, China) and the determination of protein concentration was tested by the BCA assay (KeyGen Biotech Co., Ltd., Nanjing, China). Equal amounts of protein extracts (35 μ g) were separated by 12% sodium dodecyl sulphate (SDS)-polyacrylamide gel electrophoresis (PAGE) and transferred to nitrocellulose filter (NC) membranes. The membranes were blocked in 5% non-fat milk in TRIS-buffered saline containing 0.1% Tween 20 (TBST) for 2 h at room temperature and probed with primary antibodies raised against AQP3 (Abcam, 1:800), overnight at 4°C. The membranes were washed with TBST three times. Then the membranes were incubated with horseradish-peroxidase-

conjugated antibody for 1 h at room temperature. After being washed with TBST four times, the membranes were detected by using enhanced chemiluminescence and visualized at Bio-Rad Laboratories. The Western blots shown are representative of at least three independent experiments. Densitometry of each band for the target protein was quantified by densitometry analysis with Labworks 4.6. The protein band intensity was quantified by the means \pm SEM of three experiments for each group as determined from densitometry relative to β -Tubulin (Bioworld, 1:2000).

Analysis and statistics

All of the experiments were replicated three times independently. All data were presented as the means \pm standard error mean (SEM). Statistical analysis was performed by using one-way analysis of variance (ANOVA) or t-test for data that were normally distributed. * P < 0.05 and ** P <0.01 were considered to be significant.

Function of AQP3 in the mice endometrium

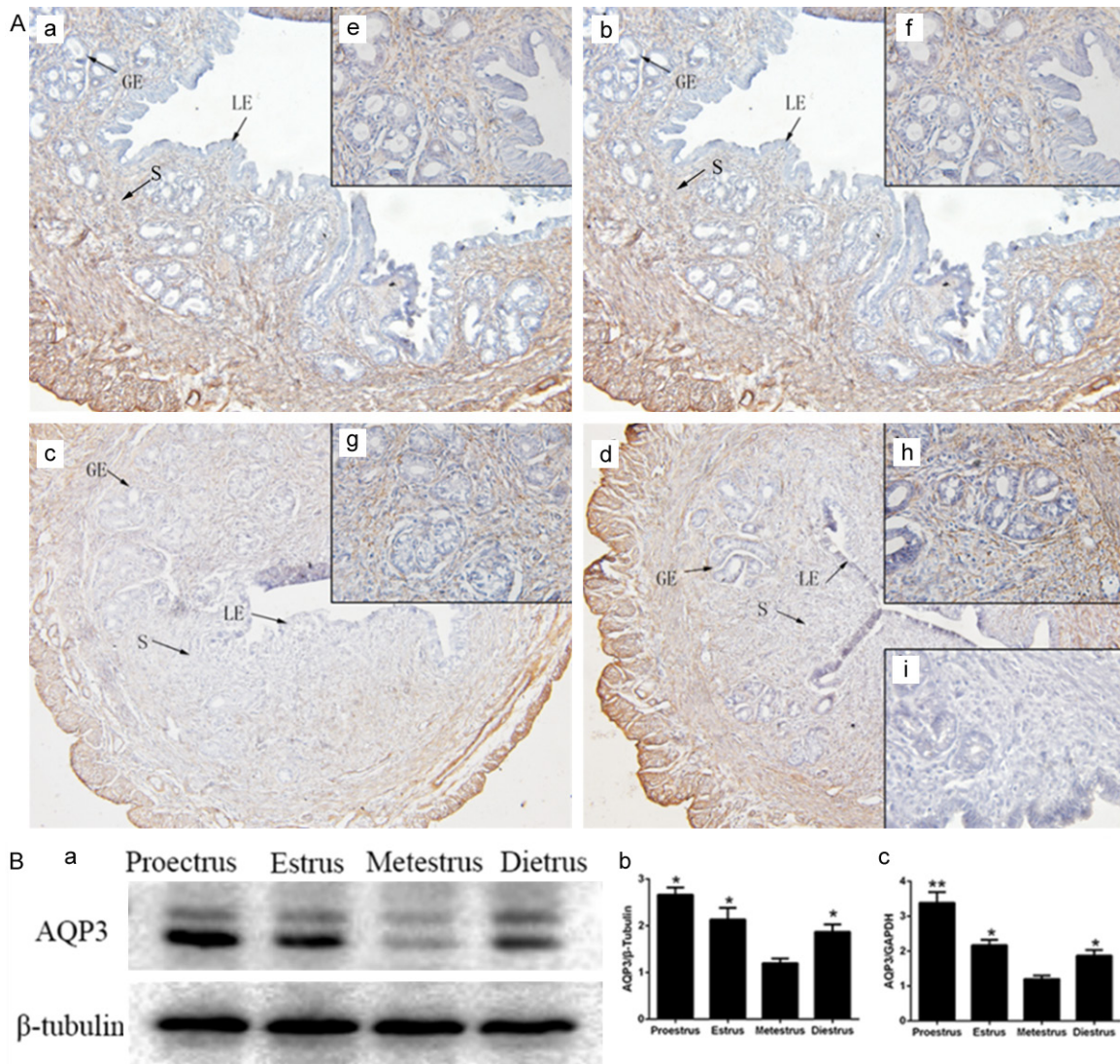


Figure 3. Expression of AQP3 in mouse uterus during estrous cycle. A. Immunohistochemical analysis of mouse uterine sections in different phases of estrous cycle using rabbit polyclonal antibody against mouse AQP3 detected AQP3 in the mouse endometrium with maximum immunostaining in the proestrus phase endometrium. Inset: Negative control of the diestrus phases (i), uterine sections stained using normal rabbit IgG. Photographs were taken with bright-field illumination. Magnification: (a-d) 100 \times ; (e-i) 400 \times . proestrus (a), estrus (b), metestrus (c), diestrus (d). stromal cells (S), glandular epithelium cells (GE), luminal epithelium cells (LE). B. (a, b) Immunoblotting analysis detected presence of AQP3 protein (32 kDa) in the total protein isolated from endometrial tissues of mice in proestrus, estrus, metestrus, diestrus phases. represents negative control where blots were probed with normal rabbit IgG; (c) The mRNA level of AQP3 expression by Real-time PCR. (* $P < 0.05$, ** $P < 0.01$).

Results

AQP3 expression varies across the estrous cycle and peaks in proestrus phase

The estrous cycle in mice of the Kunming species takes about 4-5 days. We took a vaginal smear to determine the stage of the estrous cycle, which included proestrus, estrus, metestrus and diestrus phase. This tool was a visu-

al representation of cell types and relative proportion of each cell type present during the four stages of the estrous cycle. The three cell lines included leukocyte (**Figure 1L**), cornified epithelial (**Figure 1C**), nucleated epithelial cells (**Figure 1N**) shown in the circle mark. The amount of each cell type and the relative proportion of each cell type were used to determine the stage of the estrous cycle. The vaginal

Function of AQP3 in the mice endometrium

Table 1. Expression of AQP3 protein image analysis in the mice endometrial stromal cells during estrous cycle

EC	PP	EP	MP	DP
H-score*	2.5±0.21	1.3±0.20	1.0±0.19	0.9±0.12

EC, estrous cycle; PP, proestrus phase; EP, estrus phase; MP, metestrus phase; DP, diestrus phase. Eight specimens each from different phases. *Results were expressed as the mean + SEM of H-score.

smear represented a mouse in diestrus (**Figure 1D**), with all or most of the leukocytes and a large volume of mucus. A vaginal smear with nucleated epithelial cells and a small number of leukocytes represented a mouse in proestrus (**Figure 1A**). A vaginal smear with cornified epithelial cells and a small number of nucleated epithelial cells represented a mouse in estrous (**Figure 1B**). A vaginal smear with half cornified epithelial cells and half leukocytes represented a mouse in met estrus (**Figure 1C**). Gross anatomic of uteri and immunohistochemistry showed endometrial thickening, uterine edema, and an enlarged uterine cavity gap in the proestrus and estrous of mice (**Figures 2A, 2B, 3A, 3B**). However, in the metestrus and diestrus stages, the endometrium thinned, the uterus narrowed, and the uterine cavity showed little to no gap (**Figures 2C, 2D, 3C, 3D**). Immunohistochemical results revealed the AQP3 was located in the stromal cells in the proestrus and estrous phase (**Figure 3AaS, 3AbS**), (**Table 1**), but not in the glandular epithelium (**Figure 3AaGE, 3AbGE**) and luminal epithelium (**Figure 3AaGE, 3AbGE**). To analyze the expression levels of AQP3 across the estrous cycle, we collected mice uterine endometrial tissue in the four phases of estrous cycle. The relative amounts of AQP3 mRNA were determined by performing a comparative real-time PCR analysis (**Figure 3Bc**). AQP3 transcript levels varied across the cycle. AQP3 transcript levels steadily increased from the metestrus to proestrus phase. After peaking in proestrus, AQP3 transcript levels decreased in the estrous phase. Immunoblot analysis revealed the presence of a 31 kDa band, representing the glycosylated form of AQP3 in mice uterine endometrial tissue. This trend was similar compared to the transcription levels (**Figure 3Bb**). The polyclonal rabbit anti-mouse AQP3 antibody also detected an approximately 32~34 kDa band, representing a glycosylated

form of AQP3 [19-21], on all of the blots (**Figure 3Ba**). The glycosylation was associated with increased stability and intracellular translocation of AQPs but had no influence on water permeability [22-24]. However, the 33~34 kDa band did not display differential levels.

AQP3 expression in the pregnant mouse uterus

AQP3 expression varied in the pregnant mouse uterus. We took a vaginal smear to determine estrous cycle, then female mice were cohabited overnight with fertile males. Once mating was confirmed by observing the vaginal plug the following morning (D1), female mice were euthanized at different time (D1, D5) points and uteri were collected. AQP3 transcripts were detected at D1 and D5 of pregnancy. Immunohistochemical analysis revealed intense staining for AQP3 in the stromal cells of D5 uterine tissue sections, with its localization intensely confined in the cells surrounding implantation site (**Figure 4Ab**). Spotty distribution and relatively weak immunoreactive cells were observed at D1 uterine tissue sections (**Figure 4Aa**), (**Table 2**). Low levels of AQP3 transcripts were detected at D1 compared with D5 (**Figure 4Bc**). Low levels of AQP3 protein was detected at D1 compared with D5 (**Figure 4Bab**).

AQP3 expression in the uterine stromal cells around the non-attachment site of embryo implantation

Immunohistochemical analysis results revealed that AQP3 showed no obvious expression in the uterine decidual tissue on day 8 of pregnancy (**Figure 5B, 5C, 5DZ**), or around the attachment site of embryo implantation (**Figure 4B, 4C, 4EN**). However, surprisingly, we found that AQP3 showed a specific increase in the uterine stromal cells around the non-attachment site of embryo implantation (where the uterine lumen closed down around the blastocyst) (**Figure 5A**).

Discussion

In the majority of eutherian mammals, implantation occurs in a fixed interval of time after ovulation when the corpus luteum is fully formed [25]. In humans, this is during the luteal phase of the menstrual cycle, while in rodents; it is in the estrous phase of the estrous cycle

Function of AQP3 in the mice endometrium

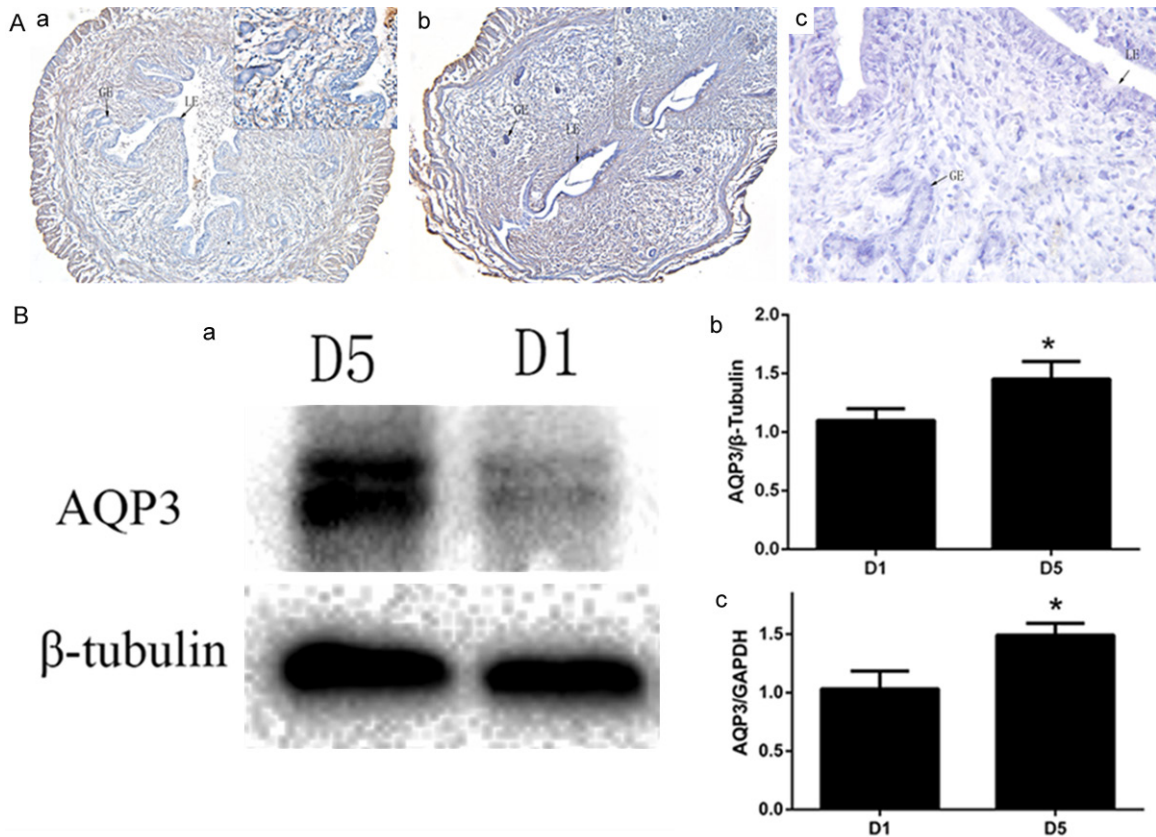


Figure 4. Expression of AQP3 in mouse uterus during early pregnancy. Female mice were cohabited overnight with stud males. Once mating was confirmed by observing the vaginal plug the following morning (D1), female mice were sacrificed at different time points and uteri were collected. Endometrial tissues were divided into 2 groups, D1 and D5. A. Immunohistochemical analysis of mouse uterine sections using rabbit polyclonal antibody against mouse AQP3 revealed intense AQP3 staining in the endometrial stromal cells at D5, (Aa) weak staining at D1, (Ab) Inset: Negative control of the D1, (Ac) uterine sections stained using normal rabbit IgG. Magnification: (Aa, Ab) 100× and insets 400×; (Ac) 400×. Stromal cells (S), glandular epithelium cells (GE), luminal epithelium cells (LE) (B) (a, b) Immunoblotting analysis of total protein isolated from the endometrial tissues of mated female mice detected AQP3 protein (32 kDa); (c) The mRNA level of AQP3 expression by Real-time PCR. (* $P < 0.05$, ** $P < 0.01$).

Table 2. Expression of AQP3 protein image analysis in the mice endometrial stromal cells during early pregnancy

EP	D1	D5
H-score*	0.98±0.21	1.6±0.19

EP, early pregnancy; Eight specimens each from different phases. *Results were expressed as the mean + SEM of H-score.

[25, 26]. The estrous cycle of mice was divided into four periods: proestrous, estrous, metestrous and diestrous. A cycle is commonly 4 to 5 days. In the diestrous phase in mice, the level of progesterone gradually increases, owing to an enhanced secretion from newly formed corpora luteum. This is accompanied by a pre-implantation surge of estrogen on day 4 of

pregnancy while embryo implantation takes place at the midnight of day 4 [26, 27].

The establishment of pregnancy is dependent on successful ovulation, fertilization, migration of the embryo to the eventual implantation site, and strict synchronization of uterine receptivity with embryonic maturation [28]. Besides the acquisition of blastocyst competency and uterine receptivity, initiation of embryo implantation also involves a timely reabsorption of intra-uterine fluids, which facilitates the apposition of embryo with the uterine endometrium. The mammalian uterus undergoes extensive morphologic changes in preparation for embryo implantation, particularly the uterine edema [29]. To better understand the mechanisms that underlie uterine edema during implanta-

Function of AQP3 in the mice endometrium

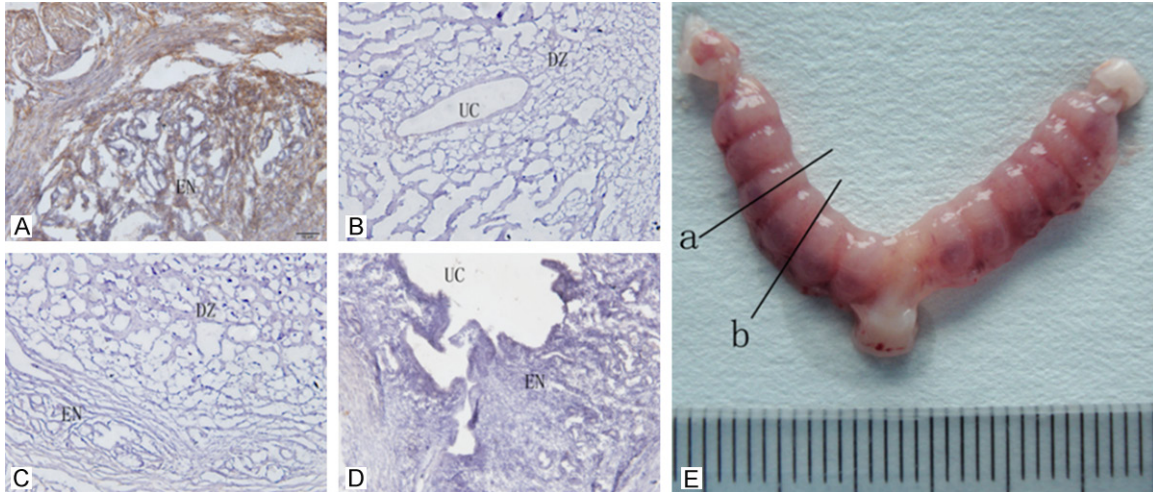


Figure 5. Expression of AQP3 in mouse uteri during the pregnancy on D8. Immunohistochemical analysis of mouse uterine sections using rabbit polyclonal antibody against mouse AQP3 detected AQP3 with immunostaining in mouse endometrium of the implantation site with embryo (A, E(b)) and without immunostaining in mouse endometrium of the implantation site without embryo and decidualization (B, C, E(a)). Inset: Negative control of mouse endometrium of the implantation site with embryo (D). EN, endometrium. UC, uterine cavity. DZ, decidual zone.

tion, we examined the expression of AQP3 water channels throughout the estrous cycle and the early weeks of pregnancy.

In this study, we demonstrated that AQP3 was located in the stromal cells, where during the proestrous and estrous phases, the endometrium thickens, uterus fills with water and uterine cavity gap enlarges. AQP3 might mediate water transport in this process, which promotes the accumulation of liquid in the uterine cavity and forming of the uterine edema. However, in the metestrous and diestrous phases, AQP3 expression decreased slightly, the endometrium thinned, the uterus narrowed, and the uterine cavity showed little to no gap. AQP3 might be responsible for water transfer out of the cavity. Overall, AQP3 might be responsible for the two-way water transfer in and out of the uterine cavity during the estrous cycle.

Water movement in the uterus is not restricted to imbibitions. Estrogen stimulates water imbibitions in the uterine endometrium. This water then crosses the epithelial cells into the lumen, leading to a decrease in viscosity of uterine luminal fluid [17]. Research indicates that the promoter of the AQP3 gene contains a functional ERE motif, which may mediate estrogen-induced up regulation of AQP3 expression [30]. Differential AQP3 expression in the uterine endometrium might be driven by the fluctuation of estrogen in estrus, affecting intrauterine fluid accumulation and uterine receptivity.

Previous studies indicated that AQP3 expression levels might relate to molecules which are important in cell-cell and/or cell-matrix interactions [30]. These studies showed a significant decrease in matrix metalloproteinases (MT1-MMP, MMP-2 and MMP-9) [31] and cell adhesion molecules (ICAM-1 [32], integrin α 5 β 1 [33] and E-cadherin [34]) after AQP3 knockdown which played an important role in the embryo implantation process. These studies also suggested that AQP3 might mediate epithelial-mesenchymal transition, suggesting that heightened levels of AQP3 expression at D5 may stimulate the expression of some matrix metalloproteinases and cell adhesion molecules, in turn, promoting the integration between the endometrium and embryo. Endometrial stroma cells decidualization initiates at the site of embryo attachment, a process that involves complex cellular changes characterized by extensive stromal cell proliferation and differentiation into decidual cells (process somewhat similar to tumor growth regarding cellular behavior and energy metabolism). Previous studies indicated that the process of uterine decidualization might utilize glycerol as an extra energy source through AQP7 (an aquaglyceroporin) facilitated glycerol transport [35]. AQP3 is also an aquaglyceroporin, but immunohistochemical results revealed that AQP3 showed no obvious expression in the uterine decidualization and endometrium on D8 of pregnancy. It is known that on day 6 of pregnancy in mice, the uterine

Function of AQP3 in the mice endometrium

lumen closes down around the blastocyst, and in the absence of a blastocyst the uterine epithelium becomes tightly apposes [36, 37]. Immunohistochemical results revealed that AQP3 showed heightened expression in the stromal cells of endometrium and the smooth muscle of the uterine tube. This led to speculation that AQP3 might mediate water out of the uterine lumen, leading to uterine contraction and ultimately a closing down of the lumen and 'tube locking'.

In summary, this study revealed that the expression of AQP3 followed a spatiotemporal pattern in the mouse endometrium during the estrous cycle and early pregnancy. High expression of AQP3 in the proestrous, estrous phase suggested that AQP3 might mediate water transport in the uterine cavity. High expression of AQP3 suggested that AQP3 might stimulate the expression of some matrix metalloproteinases and cell adhesion molecules and mediate water transport on D5 of pregnancy. High expression of AQP3 in the non-attachment site of embryo implantation and no marked expression in the attachment site suggested that AQP3 might be responsible for uterine contraction and ultimately a closing down of the uterine lumen. We found no marked expression of AQP3 in the decidual organization, therefore, AQP3 had no influence on uterine decidualization. However, further studies are planned to understand the precise mechanism underlying the role of AQP3.

Acknowledgements

This work was supported by National Natural Scientific Grants (No. 31570798), China, by the Program for Professor of Special Appointment in Liaoning Province.

Disclosure of conflict of interest

None.

Address correspondence to: Dr. Ying Kong, Department of Biochemistry and Molecular Biology, Dalian Medical University, Dalian 116044, Liaoning, China. Tel: +86-18604266169; E-mail: yingkong@dlmedu.edu.cn

References

[1] Li Y, Hu G and Cheng Q. Implantation of human umbilical cord mesenchymal stem cells for ischemic stroke: perspectives and challenges. *Front Med* 2015; 9: 20-29.

- [2] Tarara R, Enders AC, Hendrickx AG, Gulamhussein N, Hodges JK, Hearn JP, Eley RB and Else JG. Early implantation and embryonic development of the baboon: stages 5, 6 and 7. *Anat Embryol (Berl)* 1987; 176: 267-275.
- [3] Gonen T and Walz T. The structure of aquaporins. *Q Rev Biophys* 2006; 39: 361-396.
- [4] Yasui M, Hazama A, Kwon TH, Nielsen S, Guggino WB and Agre P. Rapid gating and anion permeability of an intracellular aquaporin. *Nature* 1999; 402: 184-187.
- [5] Ishibashi K, Kuwahara M, Kageyama Y, Tohsaka A, Marumo F and Sasaki S. Cloning and functional expression of a second new aquaporin abundantly expressed in testis. *Biochem Biophys Res Commun* 1997; 237: 714-718.
- [6] Liu XM, Zhang D, Wang TT, Sheng JZ and Huang HF. Ion/water channels for embryo implantation barrier. *Physiology (Bethesda)* 2014; 29: 186-195.
- [7] Tsukaguchi H, Shayakul C, Berger UV, Mackenzie B, Devidas S, Guggino WB, van Hoek AN and Hediger MA. Molecular characterization of a broad selectivity neutral solute channel. *J Biol Chem* 1998; 273: 24737-24743.
- [8] Ishibashi K, Kuwahara M, Gu Y, Tanaka Y, Marumo F and Sasaki S. Cloning and functional expression of a new aquaporin (AQP9) abundantly expressed in the peripheral leukocytes permeable to water and urea, but not to glycerol. *Biochem Biophys Res Commun* 1998; 244: 268-274.
- [9] Ishibashi K. New members of mammalian aquaporins: AQP10-AQP12. *Handb Exp Pharmacol* 2009; 251-262.
- [10] Damiano AE. Review: Water channel proteins in the human placenta and fetal membranes. *Placenta* 2011; 32 Suppl 2: S207-S211.
- [11] Sun XL, Zhang J, Fan Y, Ding JH, Sha JH and Hu G. Aquaporin-4 deficiency induces subfertility in female mice. *Fertil Steril* 2009; 92: 1736-1743.
- [12] Su W, Guan X, Zhang D, Sun M, Yang L, Yi F, Hao F, Feng X and Ma T. Occurrence of multi-oocyte follicles in aquaporin 8-deficient mice. *Reprod Biol Endocrinol* 2013; 11: 88.
- [13] Richard C, Gao J, Brown N and Reese J. Aquaporin water channel genes are differentially expressed and regulated by ovarian steroids during the periimplantation period in the mouse. *Endocrinology* 2003; 144: 1533-1541.
- [14] Lindsay LA and Murphy CR. Aquaporin-1 increases in the rat myometrium during early pregnancy. *J Mol Histol* 2004; 35: 75-79.
- [15] Lindsay LA and Murphy CR. Aquaporins are up-regulated in glandular epithelium at the time of implantation in the rat. *J Mol Histol* 2007; 38: 87-95.

Function of AQP3 in the mice endometrium

- [16] Kobayashi M, Takahashi E, Miyagawa S, Watanabe H and Iguchi T. Chromatin immunoprecipitation-mediated target identification proved aquaporin 5 is regulated directly by estrogen in the uterus. *Genes Cells* 2006; 11: 1133-1143.
- [17] Jablonski EM, McConnell NA, Hughes FJ and Huet-Hudson YM. Estrogen regulation of aquaporins in the mouse uterus: potential roles in uterine water movement. *Biol Reprod* 2003; 69: 1481-1487.
- [18] Mobasher A, Wray S and Marples D. Distribution of AQP2 and AQP3 water channels in human tissue microarrays. *J Mol Histol* 2005; 36: 1-14.
- [19] Silberstein C, Kierbel A, Amodeo G, Zotta E, Bigi F, Berkowski D, Ibarra C. Functional characterization and localization of AQP3 in the human colon. *Braz J Med Biol Res* 1999; 32: 1303-1313.
- [20] Spector DA, Wade JB, Dillow R, Steplock DA and Weinman EJ. Expression, localization, and regulation of aquaporin-1 to -3 in rat urothelia. *Am J Physiol Renal Physiol* 2002; 282: F1034-F1042.
- [21] Ikarashi N, Kon R, Iizasa T, Suzuki N, Hiruma R, Suenaga K, Toda T, Ishii M, Hoshino M, Ochiai W and Sugiyama K. Inhibition of aquaporin-3 water channel in the colon induces diarrhea. *Biol Pharm Bull* 2012; 35: 957-962.
- [22] Baumgarten R, Van De Pol MH, Wetzels JF, Van Os CH and Deen PM. Glycosylation is not essential for vasopressin-dependent routing of aquaporin-2 in transfected Madin-Darby canine kidney cells. *J Am Soc Nephrol* 1998; 9: 1553-1559.
- [23] Hendriks G, Koudijs M, van Balkom BW, Oorschot V, Klumperman J, Deen PM and van der Sluijs P. Glycosylation is important for cell surface expression of the water channel aquaporin-2 but is not essential for tetramerization in the endoplasmic reticulum. *J Biol Chem* 2004; 279: 2975-2983.
- [24] Umenishi F, Narikiyo T and Schrier RW. Effect on stability, degradation, expression, and targeting of aquaporin-2 water channel by hyperosmolality in renal epithelial cells. *Biochem Biophys Res Commun* 2005; 338: 1593-1599.
- [25] Finn CA and Martin L. The control of implantation. *J Reprod Fertil* 1974; 39: 195-206.
- [26] Wang H and Dey SK. Roadmap to embryo implantation: clues from mouse models. *Nat Rev Genet* 2006; 7: 185-199.
- [27] Zhang S, Lin H, Kong S, Wang S, Wang H, Wang H and Armant DR. Physiological and molecular determinants of embryo implantation. *Mol Aspects Med* 2013; 34: 939-980.
- [28] Cha J, Sun X and Dey SK. Mechanisms of implantation: strategies for successful pregnancy. *Nat Med* 2012; 18: 1754-1767.
- [29] Zhang Y, Chen Q, Zhang H, Wang Q, Li R, Jin Y, Wang H, Ma T, Qiao J and Duan E. Aquaporin-dependent excessive intrauterine fluid accumulation is a major contributor in hyper-estrogen induced aberrant embryo implantation. *Cell Res* 2015; 25: 139-142.
- [30] Huang YT, Zhou J, Shi S, Xu HY, Qu F, Zhang D, Chen YD, Yang J, Huang HF and Sheng JZ. Identification of Estrogen Response Element in Aquaporin-3 Gene that Mediates Estrogen-induced Cell Migration and Invasion in Estrogen Receptor-positive Breast Cancer. *Sci Rep* 2015; 5: 12484.
- [31] Xu H, Xu Y, Zhang W, Shen L, Yang L and Xu Z. Aquaporin-3 positively regulates matrix metalloproteinases via PI3K/AKT signal pathway in human gastric carcinoma SGC7901 cells. *J Exp Clin Cancer Res* 2011; 30: 86.
- [32] Tancharoen S, Matsuyama T, Abeyama K, Matsushita K, Kawahara K, Sangalungkarn V, Tokuda M, Hashiguchi T, Maruyama I and Izumi Y. The role of water channel aquaporin3 in the mechanism of TNF-alpha-mediated proinflammatory events: Implication in periodontal inflammation. *J Cell Physiol* 2008; 217: 338-349.
- [33] Kusayama M, Wada K, Nagata M, Ishimoto S, Takahashi H, Yoneda M, Nakajima A, Okura M, Kogo M and Kamisaki Y. Critical role of aquaporin3 on growth of human esophageal and oral squamous cell carcinoma. *Cancer Sci* 2011; 102: 1128-1136.
- [34] Kim NH and Lee AY. Reduced aquaporin3 expression and survival of keratinocytes in the depigmented epidermis of vitiligo. *J Invest Dermatol* 2010; 130: 2231-2239.
- [35] Peng H, Zhang Y, Lei L, Chen Q, Yue J, Tan Y and Duan E. Aquaporin 7 expression in postimplantation mouse uteri: a potential role for glycerol transport in uterine decidualization. *Fertil Steril* 2011; 95: 1514-1517.
- [36] Enders AC. Anatomical aspects of implantation. *J Reprod Fertil Suppl* 1976; 1-15.
- [37] Png FY and Murphy CR. Closure of the uterine lumen and the plasma membrane transformation do not require blastocyst implantation. *Eur J Morphol* 2000; 38: 122-127.